

Synthesis and Characterization of Lanthanum Ferrites and Their Photocatalytic Studies

K. Gurushantha^{1*}, N. Tejhaswini¹, K. S. Smitha¹, N. Sona¹, K. Sahana¹, H. Chitkala¹, Swati Verma¹ and S. Meena²

¹Department of Chemistry, M. S. Ramaiah Institute of Technology, Bengaluru - 560054, Karnataka, India; gurushanthak2016@gmail.com

²Department of Chemistry, Dayananda Sagar College of Engineering, Bengaluru - 560111, Karnataka, India

Abstract

In this fast growing environmental friendly research world, development of highly efficient, non-toxic photocatalyst for potential applications is required. Herein, a strong ability photocatalyst Lanthanum Ferrite (LF) was synthesized by solution combustion synthesis using Coconut oil (LFC) and Urea (LFU) as fuel. X-ray results indicate the development of pure phase for LF NP of perovskite structure in both the fuels having crystal size in the range of 24-48 nm. FTIR results reveal that the functional groups were confirmed. The energy band gap value from UV DRS studies was suitable for the photocatalytic degradation under visible light. The NPs displays excellent photocatalytic degradation activity for Reactive Blue 4 (RB4) dye under UV & Visible light within 120 mins resulted 75% and 84% by LFU, 89% and 98% by LFC photocatalyst respectively. LF photocatalyst has very good stability confirmed recyclability experiment for 5 cycles.

Keywords: Lanthanum Ferrites, Photocatalysis, Reactive Blue 4 Dye

1.0 Introduction

As per the recent view, the technology which received the researcher's attention for the diminution of air and water pollutants and in synthetic organic applications is photocatalysis. In this regard, various metal oxide semiconductor photocatalysts were explored recently. Titania (TiO_2) is one among this, which have potential attention due to its non-toxicity, low cost, having better chemical stability and enhanced photocatalytic activity^{1,2}. Having band gap of 3.0eV titania could possibly suitable to absorb the UV light and can able to absorb 3-5% of solar light only leads to limited practical applications³. The effective photocatalyst which got more attention and alternative to the above mentioned limitations is the perovskite structure photocatalyst having ABO_3

spinel having rare earth occupied at A and transition metal at B position⁴. Due to its spinel structure it has multi applications in all fields such as magneto-optical, dielectric, catalytic, gas-sensitive⁵⁻⁹, solid oxide fuel cell¹⁰, sensor to detect the moisture, oxygen and alcohol content^{11,12}.

The ABO_3 shows diverse property as it has the adjustable and acceptable framework to hold the various cations and defects¹³. LaFeO_3 (lanthanum ferrite) is one among the ABO_3 -spinel perovskite structure of rare earth elements orthoferrites having potential applications in the field of gas sensors, in solid oxide fuel cells as a electrodic material, in electronic and magnetic applications, in multiple catalytic activity and as electrodes in various high temperature fields^{14,15}. On the top of it, having narrow band gap and typical optoelectronic characteristics

*Author for correspondence

LaFeO₃ is identified as the efficient photocatalyst under visible light¹⁶⁻¹⁹.

Generally, the morphological crystal phase, size of the particle and band gap are the key properties for a better photocatalyst and the aforementioned properties are extremely reliant on the synthesis method. Different practical methods like sol-gel method²⁰, hydrothermal synthesis²¹, co-precipitation²², microwave assisted method²³, combustion method²⁴ from that combustion method is securing technique as it proceeded with low temperature, cost reliability and simplified process. To date, seldom any reports available on the synthesis of LaFeO₃ via solution combustion synthesis using coconut oil as fuel and the resulted material for the application in targeting at photocatalytic degradation.

In this described study, we carried out a simplified way, cost effective, less time consuming solution combustion method using urea and coconut oil as fuel in the fabrication of single-phase LaFeO₃ NPs. Further we have examined the size and structural properties of these particles by XRD and FTIR analysis. Along with degradation analysis for reactive blue 4 dye was conducted to study the photocatalytic activity of resulted NPs under UV & visible light irradiation.

2.0 Materials and Methods

The chemicals utilized for the entire study were purchased from SD Fine chemicals, Sigma-Aldrich etc. Double distilled water utilized for conduction of all experiments. For the synthesis of lanthanum ferrite, lanthanum nitrate hexahydrate (extra pure AR, 99%), Ferric nitrate nano-hydrate, urea and commercially available parachute coconut oil were used as precursors.

2.1 Synthesis

LaFeO₃ (LFO) is synthesized by solution combustion method. 9.28g La(NO₃)₃, 8.66g Fe(NO₃)₃ and 6g of urea were taken in a circular glass reactor 50 ml of double distilled water was added and stirred using magnetic stirrer at 60°C for 20 minutes. The homogeneous reaction mixture was kept in a preheated muffle furnace at 600°C in open system. Initially water solvent boils and started to evaporates, viscous solution formed. Fuel suddenly catches fire at high temperature and enormous amount

of gasses released. This process is completed around 10 minutes form voluminous powder and labeled as LFU B. The obtained powder is then calcinated at 700°C for 2 hours and labeled as LFU A. Similarly, synthesized lanthanum ferrite (LFC B & LFC A) using optimized coconut oil as a green fuel, 9.28g of La(NO₃)₃ and 8.66g of Fe(NO₃)₃ by solution combustion method.

3.0 Result and Discussion

3.1 PXRD (Powder X-ray Diffraction Method)

To determine the structural features and for the purity confirmation the XRD studies was conducted. Figure 1 depicts the XRD analysis of LFO in both fuels before and after calcination. The XRD patterns were agreeable with standard JCPDS 37-1493 without any appearance of any impure phases of La₂O₃ and Fe₂O₃ which confirms the single phase formation of LF.

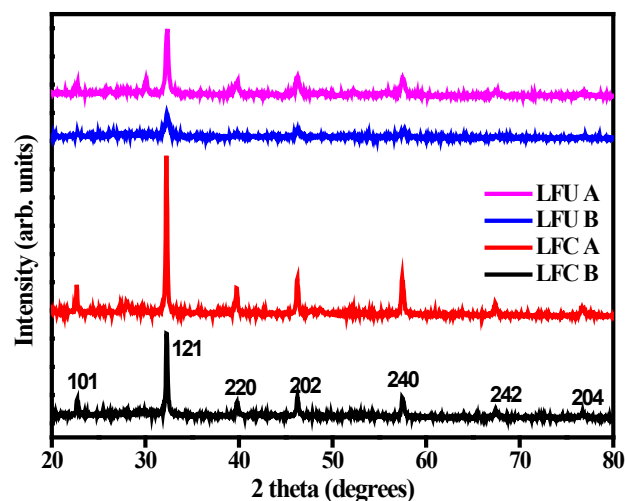


Figure 1. PXRD of Lanthanum ferrites.

Further the crystallinity of the NPs could be confirmed by the sharp diffraction patterns, the LaFeO₃ synthesized using coconut oil after calcination shows sharp peak at 32.4° of 121 plane assures the high purity of the crystal. By Debye-scherrer equation –

$$D = k \lambda / (\beta \cos\theta) \quad (1)$$

Where D = mean particle size, λ = wavelength, β = full width, θ = angle at maximum diffraction, k = shape factor

(constant) the average crystallite size is calculated for synthesized lanthanum ferrite NPs as LFCB (48.981 nm), LFCA (50.54 nm), LFUB (24.351 nm) and LFUA (31.375 nm). The calculated values indicate that the crystal size increases after calcination and crystal size is more for LFCA confirms its high crystallinity.

3.2 Diffused Reflectance Spectra

LaFeO₃ is a promising candidate for the photocatalytic activity in visible light mainly by its typical optoelectronic features with narrow energy band gap. As per the reported survey LFO shows the band gap in the range of 2.08 to 3.8 eV and this range of differences could possible arise by synthesis methods, temperature control and calcination duration, crystal size and concentration of precursors utilized²⁵. Hence the energy band gap is the dominant factor to predict the catalytic activity, the UV-DRS study was conducted.

Thus the optical band gap energy was found by the Kubelka-Munk function which relates the absorption constant and energy band as follows

$$f(R) = \frac{(1-R)^2}{2R} = \frac{k}{s} \quad (2)$$

where $R \rightarrow$ Reflectance, $f(R)$ is proportional to absorption constant of the material.

$$F(R) \propto \alpha = (h\nu - E_g)^n/h\nu \quad (3)$$

where $h \rightarrow$ Planck's constant
 $\nu \rightarrow$ frequency

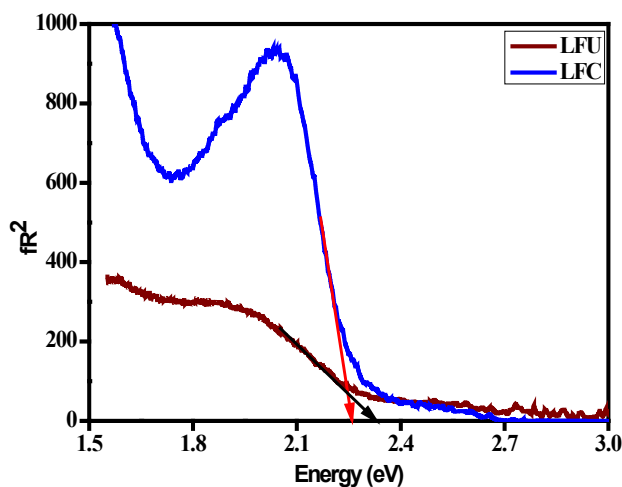


Figure 2. Diffused reflectance spectra of lanthanum ferrites.

n is 2 for indirect transitions or $\frac{1}{2}$ for direct transitions.

To identify the E_g derived from the mentioned equation the graphical plots $[F(R)h\nu]^2$ vs $h\nu$ was drawn. By extrapolating line from curve at X axis, E_g values can be evaluated (Figure 2) The resulted E_g values of LFU 2.34eV and LFC 2.25 eV are in excellent agreement with previous reported results. As the band energy gap of LFC is lesser than that of LFU, LFC acts as an effective catalyst may be due to the less energy band gap than LFU for the photo-degradation of dyes.

3.3 Fourier Transform Infrared Spectroscopy (FTIR)

The surface chemistry deals with the defects over the surface and composition plays the crucial role for photocatalytic activity. FTIR is the known characterization for the synthesized NPs to understand the control over the reaction process and the bonding properties of the elements is the materials.

Based on this criteria FTIR analysis was done by KBr pellet method to know about the bonding details in LFO NPs. The graph (Figure 3) of % transmittance v/s wavenumber in the wavenumber range (500-4000 cm^{-1}) displays the FTIR spectra. The FTIR of LFC and LFU contains the band around 3420.55 arises due to water content of O-H stretching vibration from the intermolecular H-bonding. The band around 1600 cm^{-1} might be due to C=O. The band around 550.5 cm^{-1} arises

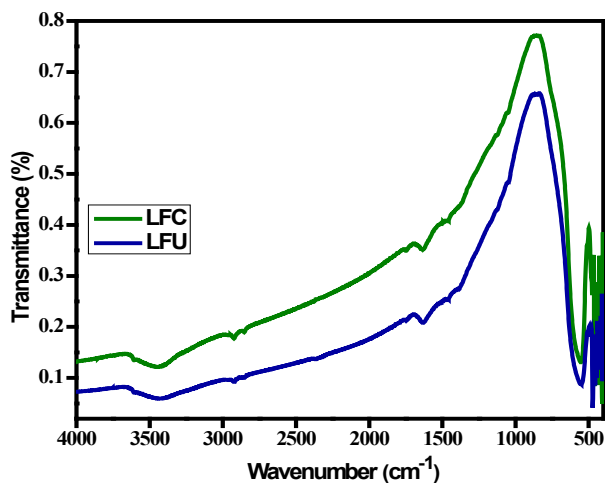


Figure 3. FTIR spectra of lanthanum ferrites.

from the bending vibrations of the metal oxide La-O bond. Metal oxides present in the samples i.e., Lanthanum oxide and ferric oxide, exhibit only the band characteristic for the vibrations of the oxides in the range of 600-400 cm^{-1} ²⁶.

3.4 Photocatalytic Activity

LaFeO_3 got more attention by the researchers due to its extraordinary photocatalytic activity as it is highly stable, non-toxic and suitable band gap. So photocatalytic activity of developed LFU and LFC was performed under UV light & visible light irradiation by taking RB4 as a model dye. The degradation of RB4 dye was ascertained by measuring the absorbance at 486 nm during the experiment.

The degradation activity for the RB4 dye was carried out by taking a suitable stock solution (10 ppm) in 100 mL distilled water along with 50 mg of the synthesized photocatalyst in a circular glass reactor. During the reaction, 4 mL of dye solution was pipetted out, centrifuged at 5000 rpm for 5 minutes to remove the catalyst and measure the absorbance using a UV-Visible spectrometer. Reactive blue 4 dye concentration reduction in photocatalyst under both UV light and visible light was monitored every 30 minutes. The outcome of this study shows the degradation activities of LFU on reactive blue 4 dye is increased with UV & Visible light irradiation time, showed excellent degradation performance and found to be 75% (UV light) & 84% (Visible light) at 120

min respectively. Similarly, experimental conditions were followed to perform degradation studies by LFC that results 89% and 98% in UV and visible light respectively (Figure 4a & b). The enhanced results of degradation by LFC might be due to its lesser band gap and high crystallinity as confirmed by UV-DRS and XRD studies.

3.5 Photocatalytic Mechanism

The feasible mechanism involved for the photocatalytic degradation of RB4 dye removal under UV/Visible radiation was proposed in Figure 5. The electrons in the valence band were excited to conduction band by UV/Visible light and same number holes leaving in conduction band (Eq. 4). The conductive oxygen vacancies existing in perovskite structure may activate the adsorbed oxygen to the surface of LFO. The photogenerated electrons react with the atmospheric oxygen to form superoxide anion radical ($\text{O}_2^{\cdot-}$) (Eq. 5). In the similar way, the generated holes react with water molecule to form hydroxide radical ($\cdot\text{OH}$) (Eq.6).

The resulted free radical react with the dye and degraded into harmless sub products (Eq.7)²⁷

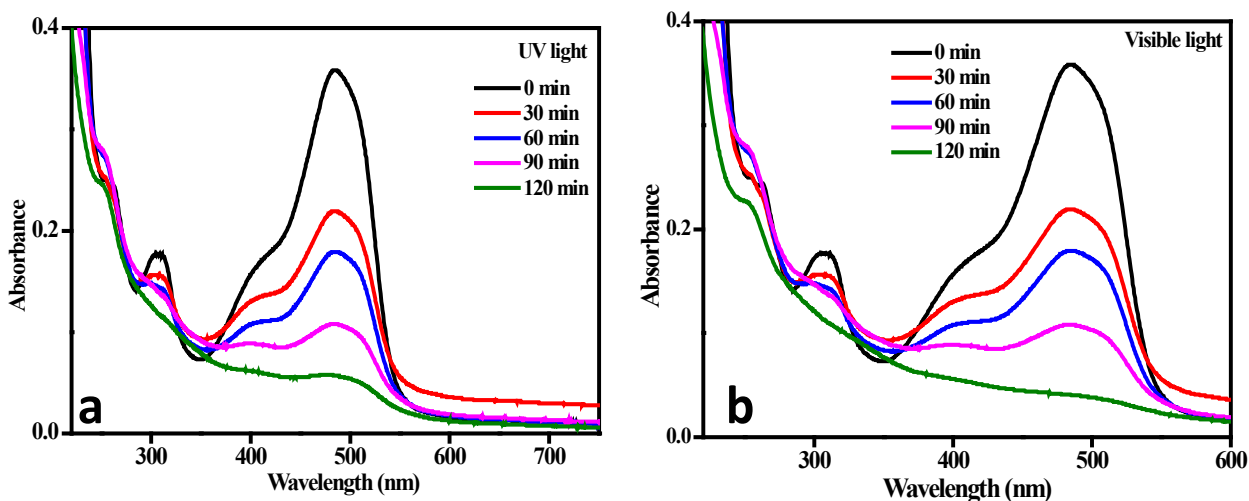
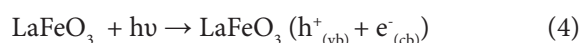


Figure 4. a) Absorbance spectra of RB4 dye in UV light b) Absorbance spectra of RB4 dye in visible light.

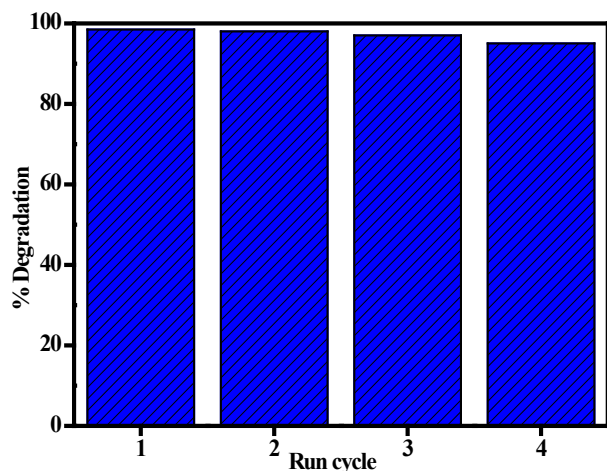


Figure 5. Recycling test of photocatalyst.

The reusability of photocatalyst is more necessary for experimental approaches. To know the reusability of synthesized NPs, 5 successive cyclic dye degradation experiments were performed using the catalyst LFC. After each cycle the catalyst can be removed by filtration technique, washed with distilled water and dried for the next cycle. The cyclic runs of the dye degradation were shown in Figure 5. The results proven that the LFC photocatalyst retains after 4 consecutive runs of experiments with meager reduction in the degradation percentage confirms that the synthesized NP is suitable for industrial applications.

4.0 Conclusion

In this present study, LFO were synthesized by solution combustion synthesis using urea as chemical fuel and coconut oil as green fuel. The effect of structure, morphology, optical properties along with the photocatalytic degradation were studied for the synthesized LFO NPs. The excellent performance of LFC NPs due to certain features like lower energy band gap, higher crystalline size with high crystallinity, were the basic reasons for excellent photocatalytic activity of 89% and 98% in UV and visible light irradiation. Finally, it is inferred from the above explanation that LFO synthesized using green fuel was found to be environmental friendly and also ahead of LFU in all the aspects which can be utilized for potential practical applications.

5.0 References

1. Chen XB, Mao SS. Titanium Dioxide Nanomaterials: Synthesis, Properties, Modifications, and Applications. *Chem Rev.* 2007; 107:2891–2959.
2. Yao N, Yeung KL. Investigation of the performance of TiO₂ photocatalytic coatings. *Chem Eng J.* 2011; 167:13–21.
3. Li M, Hong Z, Fang Y, Huang F. Synergistic effect of two surface complexes in enhancing visible-light photocatalytic activity of titanium dioxide. *Mater Res Bull.* 2008; 43:2179–2186.
4. Bae SW, Ji SM, Hong SJ, Jang JW, Lee JS. Photocatalytic overall water splitting with dual-bed system under visible light irradiation. *Int J Hydrog Energy.* 2009; 34:3243–3249.
5. Wang ZL, Kang ZC. *Functional and smart materials.* 2nd edn. New York: Plenum Press; 1998.
6. Idrees M, Nadeem M, Atif M, Siddique M, Mehmood M, Hassan M. Origin of colossal dielectric response in LaFeO₃. *Acta Mater.* 2011; 59:1338.
7. Wang Y, Wang Y, Ren W, Liu P, Zhao H, Chen J, *et al.*, Improved conductivity of NdFeO₃ through partial substitution of Nd by Ca: a theoretical study. *Phys Chem Chem Phys.* 2015; 17:29097.
8. Andoulsi R, Horchani-Naifer K, Fe'rid M. Electrical conductivity of La_{1-x}Ca_xFeO_{3-δ} solid solutions. *Ceram Int.* 2013; 39:6527.
9. El-Shaarawy MG, Rashad MM, Shash NM, Maklad MH, Afifi FA. Structural, AC conductivity, dielectric behavior and magnetic properties of Mg-substituted LiFe₅O₈ powders synthesized by sol-gel auto-combustion method. *J Mater Sci Mater Electron.* 2015; 26:6040.
10. Bidrawn F, Lee S, Vohs JM, Gorte RJ. The effect of Ca, Sr, and Ba doping on the ionic conductivity and cathode performance of LaFeO₃. *J Electrochem Soc.* 2008; 155(7):660.
11. Ciambelli P, Cimino S, De Rossi S, Lisi L, Minelli G, Porta P, *et al.* A FeO₃ (A=La, Nd, Sm) and LaFe_{1-x}MgxO₃ perovskites as methane combustion and CO oxidation catalysts: structural, redox and catalytic properties. *Appl Catal B.* 2001; 29:239.
12. Berenov A, Angeles E, Rossiny J, Raj E, Kilner J, Atkinson A. Structure and transport in rare-earth ferrates. *Solid State Ion.* 2008; 179:1090.
13. Voorhoeve R, Johnson D, Remeika J, Gallagher P. *Perovskite Oxides: Materials Science in Catalysis.* Science. 1977; 195:827.

14. Petrovic S, Terlecki A, Karanovic L, Kirilov-Stefanov P, Zduji M, Dondur V, *et al.*, LaMO₃ (M: Mg, Ti, Fe) perovskite type oxides: Preparation, characterization and catalytic properties in methane deep oxidation. *Appl Catal B*. 2008; 79:186.
15. Yoon J, Grilli M, Bartolomeo E, Polini R, Traversa E. The NO₂ response of solid electrolyte sensors made using nano-sized LaFeO₃ electrodes. *Sens Actuators B Chem*. 2001; 76:483.
16. Yang J, Zhong H, Li M, Zhang L, Zhang Y. Markedly enhancing the visible-light photocatalytic activity of LaFeO₃ by post-treatment in molten salt. *React Kinet Catal Lett*. 2009; 97:269–274.
17. Kanhere P, Nisar J, Tang Y, Pathak B, Ahuja R, Zheng J, *et al.*, Electronic Structure, Optical Properties, and Photocatalytic Activities of LaFeO₃-NaTaO₃ Solid Solution. *J Phys Chem C*. 2012; 116(43):22767-22773.
18. Acharya S, Swain G, Parida KM. MoS₂-mesoporous LaFeO₃ hybrid photocatalyst: Highly efficient visible-light driven photocatalyst. *Int J Hydrogen Energy*. 2020; 45(20):11502-11511.
19. Parida KM, Reddy KH, Martha S, Das DP, Biswal N. Fabrication of nanocrystalline LaFeO₃: An efficient sol-gel auto-combustion assisted visible light responsive photocatalyst for water decomposition. *Int J Hydrogen Energy*. 2010; 35(22):12161–12168.
20. Feng Q, Zhou J, Luo W, Ding L, Cai W. Photo-Fenton removal of tetracycline hydrochloride using LaFeO₃ as a persulfate activator under visible light. *Ecotoxicol Environ Saf*. 2020; 198:110661.
21. Phan TTN, Nikoloski AN, Bahri PA, Li D. Optimizing photocatalytic performance of hydrothermally synthesized LaFeO₃ by tuning material properties and operating conditions. *J Environ Chem Eng*. 2018; 6:1209–1218.
22. Ito K, Tezuka K, Hinatsu Y. Preparation, Magnetic Susceptibility, and Specific Heat on Interlanthanide Perovskites ABO₃ (A=La–Nd, B=Dy–Lu). *J Solid State Chem*. 2001; 157:173–179.
23. Kostyukhin EM, Kustov AL, Kustov LM. One-step hydrothermal microwave-assisted synthesis of LaFeO₃ nanoparticles. *Ceram Int*. 2019; 45:14384–14388.
24. Gurushantha K, Anantharaju KS, Renuka L, Sharma SC, Nagaswarupa HP, Prashantha SC, *et al.* New green synthesized reduced graphene oxide–ZrO₂ composite as high performance photocatalyst under sunlight. *RSC Adv*. 2017; 7:12690-12703.
25. Abazari R, Sanati S, Saghat foroush LA. A unique and facile preparation of lanthanum ferrite nanoparticles in emulsion nanoreactors: Morphology, structure, and efficient photocatalysis. *Mater Sci Semicond Process*. 2014; 25:301-306.
26. Dumitru R, Negrea S, Ianculescu A, Pacurariu C, Vasile B, Surdu A, *et al.*, Lanthanum Ferrite Ceramic Powders: Synthesis, Characterization and Electrochemical Detection Application. *Materials*. 2020; 13:2061.
27. Meena S, Anantharaju KS, Malini S, Dey A, Renuka L, Prashantha SC, *et al.*, Impact of temperature-induced oxygen vacancies in polyhedron MnFe₂O₄ nanoparticles: As excellent electrochemical sensor, supercapacitor and active photocatalyst. *Ceramics Int*. 2021; 47:14723-14740.